to be presented at IEEE/RSJ IROS, November 2013 (Tokyo)

Dynamic Surface Grasping with Directional Adhesion

Elliot W. Hawkes, David L. Christensen, Eric V. Eason, Matthew A. Estrada, Matthew Heverly, Evan Hilgemann, Hao Jiang, Morgan T. Pope, Aaron Parness and Mark R. Cutkosky

***Abstract*— Dynamic surface grasping is applicable to landing of micro air vehicles (MAVs) and to grappling objects in space. In both applications, the grasper must absorb the kinetic energy of a moving object and provide secure attachment to a surface using, for example, gecko-inspired directional adhesives. Functional principles of dynamic surface grasping are presented, and two prototype grasper designs are discussed. Computer simulation and physical testing confirms the expected relationships concerning (i) the alignment of the grasper at initial contact, (ii) the absorption of energy during collision and rebound, and (iii) the force limits of synthetic directional adhesives.**

Fig. 1. Quadrotor Micro Air Vehicle hanging from a glass surface using the directional adhesive Collapsing Truss Grasper (Sec. III-A).

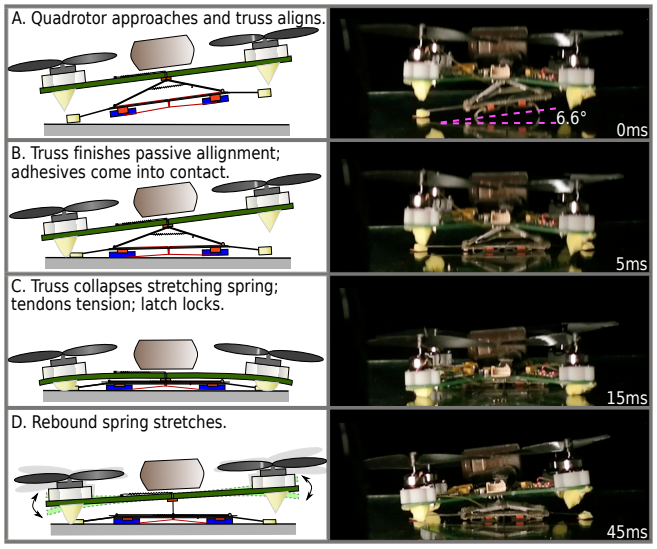

Fig. 2. A) MAV approaches surface with misalignment. B) Landing mechanism passively aligns to surface. C) Truss structure collapses to absorb energy; tendons tension to load adhesive tiles; system locks in place. D) Rebound stretches preloaded spring, which prevents overloading adhesives.

I. Introduction

The ability to grasp flat or gently curved surfaces repeatably and releasably has several compelling robotic applications including the perching of micro air vehicles (MAVs) on walls or ceilings (Fig. 1) and the grappling of orbital debris in space. In both applications, low attachment and detachment forces are required; however an important difference is that MAVs are low mass and high velocity whereas orbital debris typically has a larger mass and lower relative velocity.

Directional, gecko-inspired adhesives are suitable for these applications because they require little energy for attachment and detachment, work on many surfaces, can undergo many attach/release cycles [1], and can be scaled to either small or large applications [2]. Because the adhesives rely only on van der Waals forces to stick, they are compatible with spaceflight applications where nearly all pressure-sensitive adhesives are prohibited because of radiation, temperature and outgassing issues. Further, many of these applications require the ability to attach and release with low force, making gecko-inspired adhesives particularly appropriate.

The work presented here builds upon prior work on climbing robots, perching MAVs, and gecko-inspired adhesives. Unlike a robot climbing a wall, which can control the position, orientation and contact forces of its feet (e.g. [3], [4]), the applications considered here involve either a grasper or a target that is in free flight. The entire collision event typically lasts less than 0.1 s between initial contact and equilibrium (Fig. 2). As in other recent work [2], the devices use directional adhesives mounted to arrays of rigid tiles, loaded with central tendons. This scheme ensures that the adhesive area is loaded evenly and no moments are transferred from the device, which would cause stress concentrations and premature failure.

Previous work on MAVs that can perch on walls and other flat surfaces has exploited spines or arrays of spines [5], [6], sticky materials [7], and dry adhesives [8]. The present work is aimed at small rotorcraft that can fly at several meters per second and takes advantage of directional adhesives capable of sticking and releasing rapidly and with very low effort [1], [9]. Work on the control of MAVs in confined spaces (e.g. [10], [11], [12], [13]) is also relevant for establishing the range of velocities and orientations that may be expected

E. W. Hawkes, D. L. Christensen, M. A. Estrada, H. Jiang, M. T. Pope, and M. R. Cutkosky are with the Dept. of Mechanical Engineering, Stanford University, Stanford, CA 94305, USA ewhawkes@stanford.edu

E. V. Eason is with the Dept. of Applied Physics, Stanford University, Stanford, CA 94305, USA easone@stanford.edu

M. Heverly, E. Hilgemann and A. Parness are with the Robotic Vehicles and Manipulators Group, NASA JPL, Pasadena, CA 91109, USA Aaron.Parness@jpl.nasa.gov

at contact.

The problem of space debris is increasingly of concern to space agencies around the world. There are currently over 1500 rocket bodies and over 10,000 other debris objects in Earth orbit [14]. In 2007, a piece of debris collided with an active communication satellite causing a total loss worth many millions of dollars in damage. With the mechanisms presented here, "non-cooperative" targets can be acquired, in contrast to previous systems which have relied on pre-installed grapple features on cooperative targets. For example the arms on the Space Shuttle and the International Space Station. Similarly, the Orbital Express mission demonstrated docking with a cooperative target [15], [16]. The FREND arm is planned for use aboard the DARPA Phoenix mission and is expected to grasp a non-cooperative target using a Marman Clamp, a fixed hard point on the side of the spacecraft [17]. The devices presented here do not require specialized fixtures and can attach to flat or gently curved smooth surfaces including solar panels and the sides of spacecraft, fuel tanks, etc. They have the potential to simplify orbital debris clearance, making it more robust and less reliant on precision sensing and navigation.

The following section of this paper presents a set of functional principles for grasping surfaces under dynamic conditions, when either the grasper or target is in free flight. Next, prototype designs embodying these principles are described. Modeling and testing results show that these designs are capable of absorbing collision energy and using it to align the surfaces and apply loads to the directional adhesives, causing them to attach without bouncing away. The paper concludes with a discussion of ongoing work to incorporate these prototypes into MAVs and into space grappling devices for environment testing to simulate orbital conditions [18].

II. Functional Principles

Grasping a surface dynamically requires several properties for the gripper, whether for perching MAVs on a surface in Earth's gravity or grappling a target in space. This section generalizes the problem of dynamic surface grasping and describes several functional principles that must be embodied by a gripper using directional adhesives.

A. Dynamic Passive Alignment

When the grasper first makes contact with the surface, it is unlikely that the adhesive tiles will be aligned. Hence the grasper must compensate for misalignment before or during the collision (Fig. 3, *A*). A passive alignment system can be lighter, simpler, and more robust than an actuated system.

For a passive system, it is important that the work required for alignment is small compared to the grasper's kinetic energy in order to prevent rebounding before alignment has occurred. The system should therefore have low moments of inertia and rotational stiffnesses.

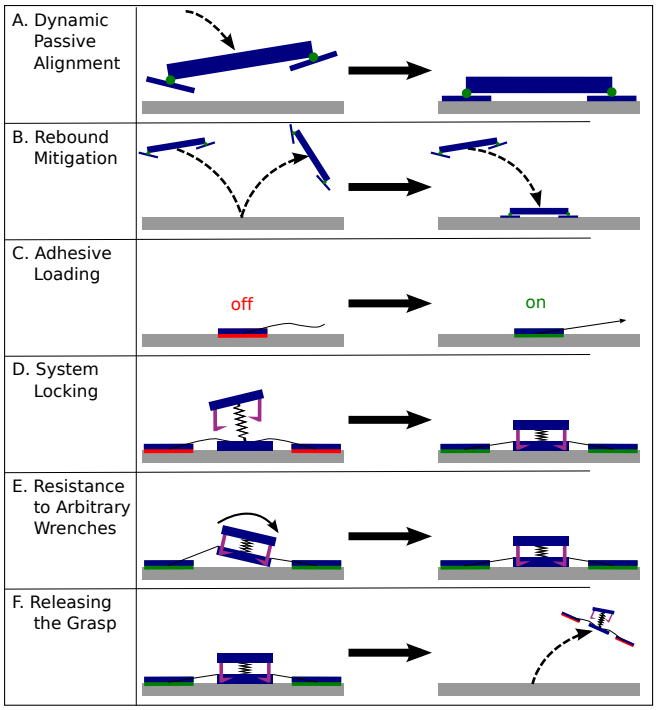

Fig. 3. Illustration of the Functional Principles described in Sec. II.

B. Rebound Mitigation

The remaining kinetic energy of the grasper must be absorbed during the collision or during rebound (Fig. 3, *B*). The maximum energy that can be absorbed is limited by the size of the device and the energy absorbing force. The energy absorbing force is itself limited. During collision, it must not damage the device; and during rebound, it must not exceed the adhesion limits of the adhesive tiles.

C. Adhesive Loading

Unlike pressure sensitive adhesives, directional adhesives are not sensitive to normal preload [19]: simply pressing them into the surface will not make them stick. Directional adhesives produce negligible adhesion unless shear force is applied in the correct direction to turn the adhesive "ON" (Fig. 3, *C*). In order to support normal loads without shear, the grasper must use multiple tiles of directional adhesive which are loaded with internal shear forces in opposing directions.

With an appropriate mechanism, the energy of the collision can be exploited to passively create these forces and turn the adhesives "ON" at the appropriate time. Excessive shear force will cause the directional adhesives to fail, so the mechanism must ensure the shear force lies within acceptable limits. The excess energy must be dissipated or stored elsewhere. Alternatively, the forces may be produced by an active mechanism. All adhesive tiles must be aligned and in contact with the surface before the adhesives are loaded, so an active mechanism must have accurate sensing to ensure correct timing.

D. System Locking

Once the internal shear force has been applied to the adhesives and as much energy as possible has been absorbed during the collision, the grasper must enter a locked state to keep the internal shear forces in place and store the absorbed energy. (Fig. 3, *D*). This can be achieved passively using a ratchet or latch.

E. Resistance to Arbitrary Wrenches

The grasper must be able to support arbitrary wrenches, i.e. combinations of applied forces and moments (Fig. 3, *E*). Ideally, the grasper mechanism should distribute these loads optimally to limit the maximum force on the adhesive, so that the grasper's force limit equals the combined force limits of the separate individual adhesive tiles.

This is not straightforward because the tiles are initially misaligned on the surface, and their positions change during the collision. Therefore, the grasper mechanism must compensate by taking up any slack in the loading tendons, and it must distribute loads optimally despite this compensation.

F. Releasing the Grasp

For directional adhesives, it is not necessary to apply a detachment force. When releasing the grasp is desired, a release mechanism can disengage the system lock to release the internal shear loads and turn the adhesives "OFF." This allows the stored energy, if any, to push the surface and grasper apart (Fig. 3, *F*).

III. Design

Two designs are presented that display the functional principles of dynamic surface grasping. The first, a collapsing truss design, is sized for use on a MAV. The second, a pivoting linkage design, has been sized and fabricated both for use on a MAV and as a prototype for future use in Earth orbit to grapple orbital debris.

A. Collapsing Truss Grasper

This grasper design is based on a collapsing truss mechanism (Fig. 4). It is designed as low-mass landing gear (3.5 g) for a 120 g MAV, and uses 2 adhesive tiles (1×1 cm square). To decrease the pitch-back moment when the MAV is attached to a wall, the Collapsing Truss Grasper is designed to be low profile in the collapsed position. The grasper is designed in accordance with the functional principles presented in Sec. II.

The truss is attached to the MAV at its apex by a single tendon which passes through a compliant foam joint, which keeps the grasper aligned to the MAV during flight but allows it to rotate and translate during a collision. Translation is necessary because one tile of adhesive makes contact before the other, and the tiles resist sliding. The grasper uses a set of outriggers to decrease the alignment force and ensure it is partially aligned before contact (**Dynamic Passive Alignment**). A model of this alignment system is described in Sec. IV-A.

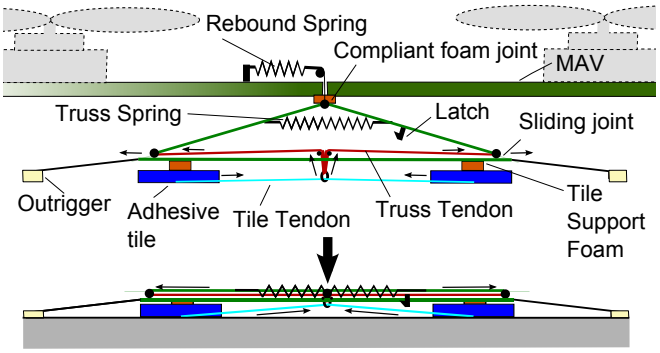

Fig. 4. Collapsing Truss Grasper. A) Schematic showing functional components. B) Device in locked state (grasping a surface).

As the truss collapses, the Truss Tendon routed between the two legs of the truss becomes taut. This pulls the center of the Tile Tendon against the bottom of the truss, applying shear forces to the adhesive tiles and turning them "ON." The internal shear force is limited by the length of the Truss Tendon (**Adhesive Loading**). Energy is absorbed during the collision by the Truss Spring. When the truss collapses fully, a latch engages to lock the truss in the collapsed state (**System Locking**). If desired, the Truss Spring can be removed to minimize the amount of normal force required to collapse the truss. Extra energy is absorbed by the Rebound Spring, which is attached to the tendon through the compliant foam joint (**Rebound Mitigation**). This spring is preloaded in order to keep the truss pulled tight to the MAV and because a preloaded spring can absorb more energy in this situation (see Sec. VI-C).

Once the grasper is locked in place, the Tile Tendon remains under tension and stays at an essentially constant angle, geometrically defined by the length of the Tile Tendon and the distance between the tiles. When a large external load is applied (e.g. wind on the MAV), this load is distributed between the two tiles and additional tension is applied to the Tile Tendon, adding more internal shear force, which produces more adhesion due to the directional nature of the adhesives (**Resistance to Arbitrary Wrenches**). The Tile Tendon angle can be fine-tuned to change the performance characteristics of the grasper, as described in Sec. IV-B.

B. Pivot Linkage Grasper

The other grasper design uses a pivoting linkage to apply tension to the Tile Tendons. Unlike the Collapsing Truss Grasper, the adhesive tiles are loaded with semi-independent mechanisms, so the Pivot Linkage Grasper can have a larger number of adhesive tiles. Two versions of this design are presented, each using 4 adhesive tiles: The MAV Pivot Linkage Grasper is designed as landing gear for a 120 g MAV and uses 1×1 cm square adhesive tiles (Fig. 5); and the Space Pivot Linkage Grasper is designed as a prototype for grappling operations in Earth orbit and uses 4×4 cm square adhesive tiles (Fig. 6).

The mechanisms are actuated by pressing the Center Plate and the Baseplate together. This causes the Tensioning Arms

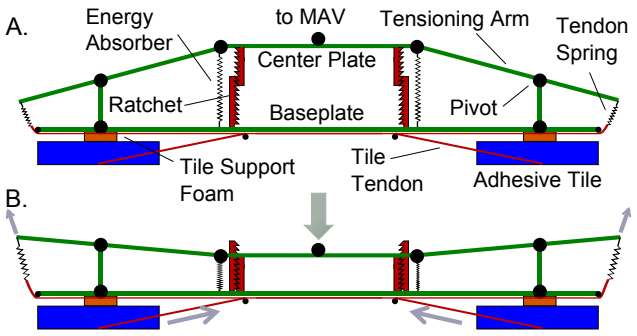

Fig. 5. MAV Pivot Linkage Grasper. A) Schematic showing functional components. B) Device in locked state (grasping a surface).

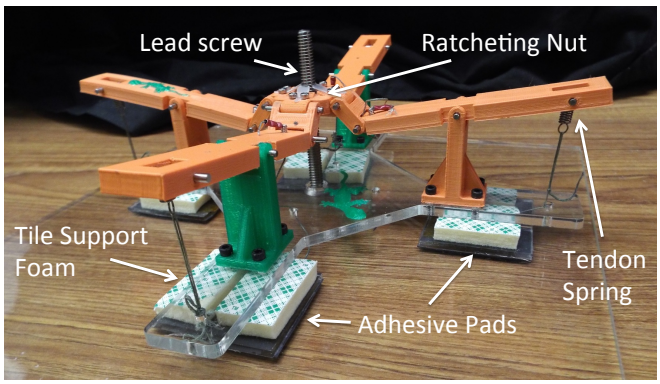

Fig. 6. Space Pivot Linkage Grasper shown in the locked state (grasping a surface).

to rotate around the Pivots and apply force to the Tile Tendons through the Tendon Springs. The MAV version uses tendons that pull inwards, crossing under the center of the Baseplate for compactness, while the Space version uses tendons that pull outward to enable grasping flexible surfaces such as thermal blankets.

The MAV Pivot Linkage Grasper uses the energy of collision to turn "ON" the adhesive tiles. It requires a larger normal preload force than the Collapsing Truss Grasper to apply the internal shear forces to the adhesive tiles. This is partly because it has less mechanical advantage, but also because the system of 4 tiles is over-constrained and therefore some amount of preload is necessary to deflect the Tile Support Foam and bring all tiles into contact. Once the tiles make contact, the Tendon Springs compensate for any initial misalignment of the adhesive tiles. In the MAV grasper, the Tendon Springs are preloaded and nonlinear, producing a nearly constant force over a large range of deflection to ensure that all 4 tiles are loaded evenly throughout the collision.

The Space Pivot Linkage Grasper works similarly but can also function in absence of a collision by turning the Leadscrew. This actively applies the shear load to the adhesive tiles without requiring a normal force, so preload is only required to deflect the Tile Support Foam. In the Space grasper, the Tendon Springs are linear, but the Leadscrew allows the grasper to control the tension as necessary: for example, a lower tension could be used when grasping a rougher surface to prevent the adhesives from failing prematurely, but a higher tension could be used on a smoother surface to increase the grasper's loadbearing capacity.

Kinetic energy is absorbed by the Energy Absorbers and locked in place using ratchets or a Ratcheting Nut. These ratchet systems may lock at multiple points, which allows the Pivot Linkage Graspers to absorb a variable amount of energy during different collisions (unlike the Collapsing Truss Grasper). In addition, the Energy Absorbers have nonlinear stiffness to provide maximum deceleration in a short distance (Sec. VI-C). A rebound spring may be added to the MAV grasper to absorb additional energy; alternatively, the Space grasper is intended to be mounted on a compliant robotic arm which may be used for active rebound mitigation.

After a Pivot Linkage Grasper is locked and external loads are applied, the Tile Tendons behave as if they were inextensible. This is because the Tendon Springs do not stretch or relax until the external load is high enough to balance the external work with the energy change in the springs. Since the Tile Tendons do not change length or tension, the applied loads are instead reacted by changes in Tile Tendon angle and corresponding deflections of the Tile Support Foam.

IV. Modeling

A. Collapsing Truss Grasper: Passive Alignment

In order for a passive alignment strategy to work, the grasper must be fully aligned to the surface before any tension is applied to the Tile Tendons. For the Collapsing Truss Grasper, this means the outriggers must apply enough force to overcome the rotational inertia before the adhesive tiles contact the surface, while not applying enough force to cause the truss to begin to collapse.

In order to obtain a better understanding of the passive alignment process, the equations of motion of this system were modeled in Motion Genesis™, using the dimensions and material properties of the physical Collapsing Truss Grasper. Simulation results are shown in Fig. 7. For the combination of initial conditions seen in high speed video screenshots of Fig. 2, the simulation predicts that the grasper aligns to the wall before the adhesive tiles contact the surface. The maximum reaction force at the apex of the truss is about 0.38 N, which is lower than the force required to collapse the truss, or 0.59 N. Thus the passive alignment process completes before the truss collapses, which is also verified by high speed video.

B. Collapsing Truss Grasper: Adhesive Loading

The behavior of a directional adhesive can be described by a limit curve in force space, which is the locus of normal and shear stresses that the adhesive can support before failure [20], [19]. The limit curve of a grasper mechanism, however, is a different shape than the limit curves of the individual adhesive tiles (for instance, the grasper can support pure normal loads while the adhesive tiles cannot).

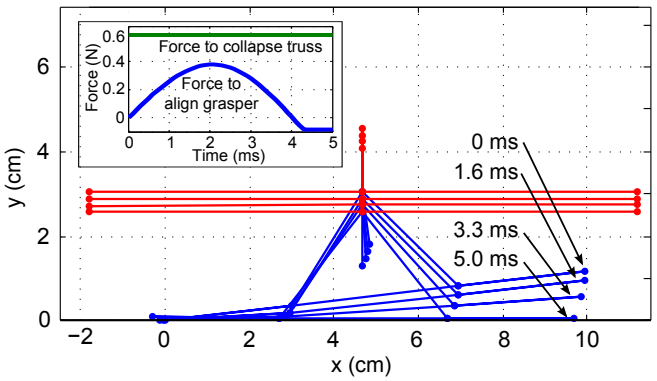

Fig. 7. Wireframe animation of simulated grasper model during passive alignment with incoming velocity 1 m/s and angular misalignment 6.6°. Inset: reaction force at apex of grasper (blue). Force to collapse truss shown for comparison (green).

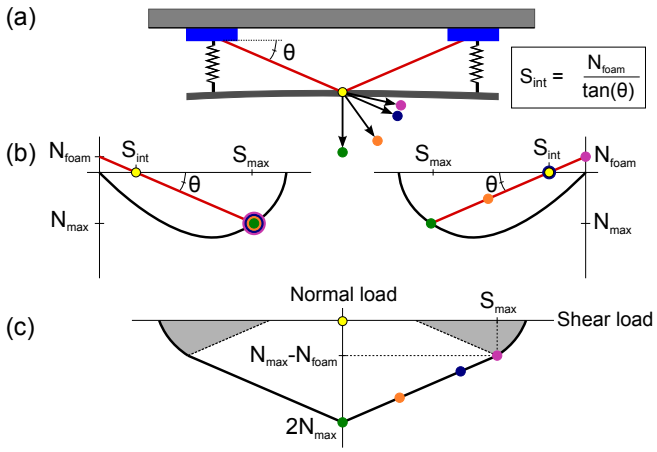

Fig. 8. (a) Simple model of the collapsing truss grasper. (b) Individual limit curves of the two opposed tiles. (c) Predicted combined limit curve of the collapsing truss grasper.

In the case of the Collapsing Truss Grasper, a simple model can be created to find the grasper limit curve using the two adhesive tiles' limit curves. The model is shown in Fig. 8a. The load on the tiles is the resultant of the tension force along each Tile Tendon at angle θ and the compressive force through each Tile Support Foam piece. Since the geometry is fixed (the tendons are inextensible), the foam pieces produce a constant force N_{foam}, and the forces on the tiles are constrained to lie along a line segment in force space with angle θ and intercept N_{foam}, and which intersects the limit curve at the point (S_{max}, N_{max}), as shown in Fig. 8b.

If the assumption of constant geometry is valid, the combined limit curve of the grasper mechanism is the direct sum of these line segments, which is a rhombus-shaped region in force space (Fig. 8c). Along the lower edges of this rhombus, one of the tiles is at its maximum load (S_{max}, N_{max}) while the other is somewhere else on the line segment of possible loads. The maximum normal load for the grasper is $2N_{max}$.

Adjacent to the upper edges of the rhombus are regions in force space where one of the Tile Tendons is no longer in tension. This does not necessarily mean grasper failure, but the geometry is no longer expected to be constant so this simple model is no longer accurate. These regions are shaded gray in Fig. 8c.

V. Fabrication

The MAV graspers are fabricated using fiberglass and acetal laser-cut parts, carbon fiber rods, silicone open-cell foam, and kevlar braided cord. The Collapsing Truss Grasper has dimensions 50×20×8 mm in the locked state. The Space grasper is fabricated using 3-D printed parts (fused filament fabrication), laser cut acrylic, braided line and other off the shelf components.

The directional adhesive used in these mechanisms is fabricated by casting PDMS silicone into a mold created using a photolithographic process [1]. This produces a 300-400 μm thick film with an array of 80 μm tall angled micro-wedges. A thin, smooth PDMS film is then deposited on the tips of the features through a post-treatment process involving dipping them into uncured PDMS and then pressing them against a wafer [9], causing a change in shape and surface smoothness on the engaging surfaces. After post-treatment, the back side of the film is glued to a fiberglass sheet using RTV silicone adhesive (Smooth-On Sil-Poxy), and the fiberglass sheet is then cut into tiles using a laser cutter. Tendons made of kevlar braided cord are attached to the front center of the tiles and routed through rectangular cutouts, in a similar design to adhesive tiles developed previously [2].

VI. Results

A. Collapsing Truss Grasper: Limit Curves

The limit curve of one of the adhesive tiles used in the Collapsing Truss Grasper was measured using a motorized positioning stage and a six-axis force-torque transducer, using methods described in [9]. This limit curve is plotted in Fig. 9, A. Note that the limit curve goes through the origin, indicating that no adhesion is produced without shear force.

By drawing a line segment in Fig. 9, A at the angle of the tendons (measured to be θ = 13 deg), approximate values of $S_{max} = 4$ N and $N_{max} = 1$ N can be determined. Based on the simple model of Fig. 8, it is predicted that the grasper's combined limit curve will have a maximum normal force of $2N_{max} = 2$ N and a maximum shear force of $S_{max} = 4$ N (or more). Next, the combined limit curve of the grasper was also measured; the resulting data are shown in Fig. 9, B. While there is some amount of asymmetry due to variations between the two adhesive tiles, the maximum normal and shear forces agree well with the predictions from the simple model.

B. Collapsing Truss Grasper: Preload

The maximum adhesion of the Collapsing Truss Grasper with varying amounts of normal preload was measured by pressing the grasper into a glass surface using weights of various sizes, and then pulling the grasper perpendicularly off the surface and recording the maximum normal force.

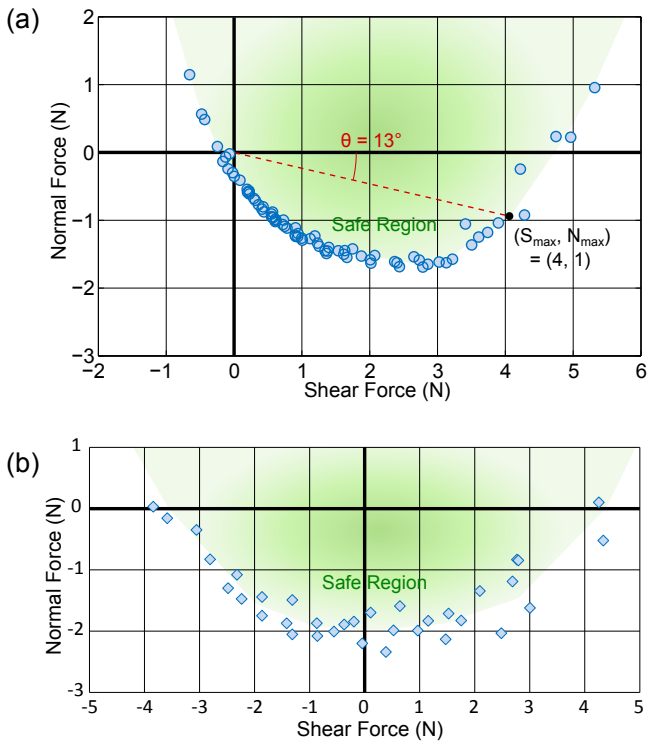

Fig. 9. A) Measured limit curve of a single 1×1 cm adhesive tile used in the collapsing truss grasper. Adhesive forces are plotted as negative values. B) Measured limit curve of the collapsing truss grasper, which uses two 1×1 cm adhesive tiles.

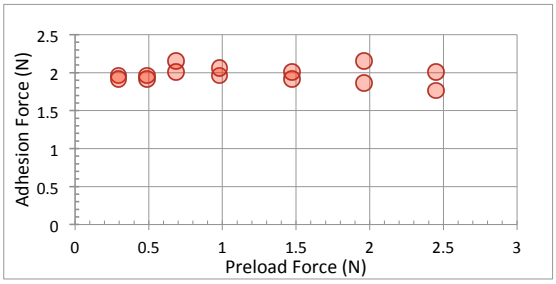

Fig. 10. Graph showing the amount of adhesion force generated versus normal preload force applied for the collapsing truss grasper. The adhesion force is independent of preload beyond some very small threshold.

The Truss Spring was removed for this test to decrease the force required to collapse the truss. This removes the capability of the device to absorb energy during collision, but this would be acceptable in a low-energy application. The test data, plotted in Fig. 10, indicate that the normal preload has no observable effect on the maximum adhesive load: the grasper can be used with any preload in the range of 0.3 to 2.4 N with an essentially constant normal adhesion (2 N). However, a preload smaller than 0.3 N is not sufficient to engage the mechanism's latch. The adhesive tiles themselves appear to be very insensitive to preload, as has been previously shown [19].

C. MAV graspers: Energy absorption

An experiment was conducted to investigate energy absorption during collision. The MAV Pivot Linkage Grasper

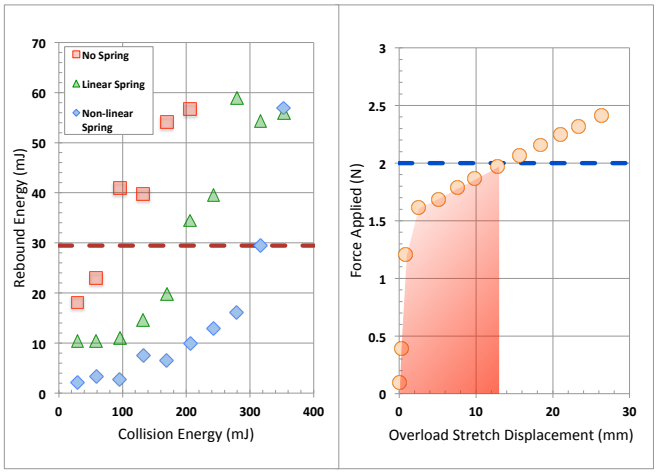

Fig. 11. Left: Rebound energy vs. collision energy for three different energy absorbing configurations. Right: Force vs. displacement of the Rebound Spring.

was tested by dropping it onto a surface and measuring the rebound height (the adhesives were removed for this test). This experiment was repeated with different incoming kinetic energies and with three different Energy Absorbing configurations: linear springs with a ratchet, nonlinear springs (near constant-force) with a ratchet, and no springs. These data are plotted in Fig. 11, left.

For nearly all incoming kinetic energies tested, the rebound energies of the three configurations were in a specific order, with the no-spring configuration being highest and the nonlinear spring being lowest. This indicates that the nonlinear spring absorbs the most energy during collision of all the energy absorbing configurations.

To compare this energy with the energy absorbed during rebound, a force vs. displacement curve was measured for the Rebound Spring used by the MAV graspers (Fig. 11, right). Given the maximum normal load the grasper can support (e.g. 2 N for the Collapsing Truss Grasper), the maximum permissible rebound energy is the integral of the curve up to the maximum load (red region in Fig. 11), which is approximately 29 mJ. This energy is plotted as a red dashed line in Fig. 11, left. This plot can be used to approximate the maximum permissible incoming kinetic energy for the three damping configurations, with the result that the nonlinear spring allows nearly twice as much kinetic energy as the linear spring and 4 times as much as no spring.

D. Pivot Linkage Grasper: Scalability and Dynamic Capture

The scalability of grasper designs was investigated by testing the Space Pivot Linkage Grasper at higher loads. Pull tests were performed on a variety of surfaces using a digital force gauge. Successful grasping was demonstrated on a variety of surfaces including satellite solar panels. A maximum normal adhesive force of >60 N was demonstrated. Tests were also performed to verify the load-sharing function of the tendons with carefully selected tiles. The normal adhesion of the grasper was found to be four times as large as the lowest-performing tile. When a set of opposing tiles were

intentionally separated from the surface, hard stops in the mechanism allowed the remaining two tiles to demonstrate a contact strength of twice the lowest-performing tile.

Dynamic capture tests were performed with a human holding the grasper system in place of the FREND robotic arm that will be used in future testing [17]. Using a simulated piece of debris (a 33 kg foot locker with wheels and several space-like surfaces mounted), capture experiments were performed at a variety of relative velocities and spin rates. The maximum successful capture had relative motion of over 2 m/s and a spin rate of $>$75 deg/s. This demonstration is included in the paper's accompanying video.

VII. Conclusion

The surface grasper designs developed here are practical and effective, as seen in the demonstration video accompanying this paper. Their performance in real-world tests is in line with expectations, and their behavior matches well with simple models. The functional principles presented in Sec. II will be useful to inform grasper designs in the future. New designs or iterations of the present designs can enable flying robots to land on arbitrary surfaces and spacecraft to perform orbital debris cleanup, as well as any other application where sticking and un-sticking to a smooth surface is desired.

VIII. Future Work

While there has been initial success grasping a surface during flight with a controlled vehicle using a MAV grasper, it remains to be done to probe the landing envelope to learn what combination of incoming velocities and misalignments are acceptable. Beyond this, automating the grasp release and achieving a transition back to flight will be a future goal.

Future experiments with space graspers are planned for a large air bearing surface in the next several months. Using a robotic arm, the grasper mechanism will be integrated into a realistic grappling scenario that mimics the microgravity environment in Earth's orbit. Characterization of the grasper's performance over a range of spin and tumble rates will be performed using a Vicon motion capture system. This venue will also allow system integration with impedance control on the arm and several computer vision algorithms.

IX. Acknowledgments

Research was carried out, in part, at the Jet Propulsion Lab, California Institute of Technology, under contract with the National Aeronautics and Space Administration. Government Sponsorship Acknowledged. The views expressed are those of the author and do not reflect the official policy or position of the Department of Defense or the U.S. Government. Approved for Public Release, Distribution Unlimited. The work of E. W. Hawkes, M. A. Estrada, and E. V. Eason was supported by the National Science Foundation Graduate Research Fellowship Program. E. V. Eason is additionally supported by the Stanford Graduate Fellowship Program and the Hertz Foundation.

References

[1] A. Parness, D. Soto, N. Esparza, N. Gravish, M. Wilkinson, K. Autumn, and M. Cutkosky, "A microfabricated wedge-shaped adhesive array displaying gecko-like dynamic adhesion, directionality and long lifetime," *J. Royal Society, Interface*, vol. 6, no. 41, pp. 1223–1232, Mar 2009.

[2] E. Hawkes, E. Eason, A. Asbeck, and M. Cutkosky, "The gecko's toe: Scaling directional adhesives for climbing applications," *Mechatronics, IEEE/ASME Transactions on*, vol. 18, no. 2, pp. 518–526, 2013.

[3] S. Kim, M. Spenko, S. Trujillo, B. Heyneman, D. Santos, and M. Cutkosky, "Smooth Vertical Surface Climbing With Directional Adhesion," *IEEE Trans. on Robotics*, vol. 24, no. 1, pp. 65–74, 2008.

[4] M. Murphy, C. Kute, Y. Menguc, and M. Sitti, "Waalbot II: Adhesion Recovery and Improved Performance of a Climbing Robot using Fibrillar Adhesives," *The International Journal of Robotics Research*, vol. 30, no. 1, pp. 118–133, 2011.

[5] M. Kovac, J. M. Germann, C. Hurzeler, R. Siegwart, and D. Floreano, "A perching mechanism for micro aerial vehicles," *Journal of Micro-Nano Mechatronics*, vol. 5, pp. 77–91, 2009.

[6] A. Lussier-Desbiens, A. T. Asbeck, and M. R. Cutkosky, "Landing, perching and taking off from vertical surfaces," *IJRR*, vol. 30, no. 3, pp. 355–370, 2011.

[7] M. L. Anderson, C. J. Perry, B. M. Hua, D. S. Olsen, J. R. Parcus, K. M. Pederson, and D. D. Jensen, "The sticky-pad plane and other innovative concepts for perching uavs," in *47th AIAA Aerospace Sciences Meeting*, 2009.

[8] L. Daler, A. Klaptocz, A. Briod, M. Sitti, and D. Floreano, "A perching mechanism for flying robots using a fibre-based adhesive," in *IEEE ICRA*, 2013.

[9] P. Day, E. Eason, N. Esparza, D. Christensen, and M. Cutkosky, "Micro-wedge machining for the manufacture of directional dry adhesives," *Journal of Micro and Nano-Manufacturing*, 2013 (in press).

[10] N. Michael, D. Mellinger, Q. Lindsey, and V. Kumar, "The GRASP multiple micro UAV testbed," *IEEE Robotics and Automation Magazine*, vol. 17, pp. 56–65, September 2010.

[11] D. Mellinger, N. Michael, and V. Kumar, "Trajectory generation and control for precise aggressive maneuvers with quadrotors," *The International Journal of Robotics Research*, vol. 31, no. 5, pp. 664–674, April 2012.

[12] A. M. Hyslop and J. S. Humbert, "Autonomous Navigation in 3-D Urban Environments Using Wide-Field Integration of Optic Flow," *AIAA Journal of Guidance, Control, and Dynamics*, vol. 33, no. 1, pp. 147–159, 2010.

[13] E. Glassman, A. Lussier-Desbiens, M. Tobenkin, M. Cutkosky, and R. Tedrake, "Region of Attraction Estimation for a Perching Aircraft: A Lyapunov Method Exploiting Barrier Certificates," *IEEE International Conference on Robotics and Automation*, pp. 2235–2242, May 2012.

[14] "Orbital debris quarterly news," NASA Orbital Debris Program Office, pp. 1–10, Apr 2009.

[15] D. A. Whelan, E. A. Adler, S. B. Wilson III, and G. M. Roesler, Jr., "DARPA orbital express program: effecting a revolution in space-based systems," *SPIE Small Payloads in Space*, vol. 4136, pp. 48–56, 2000.

[16] R. Friend, "Orbital express program summary and mission overview," *Proc. of SPIE, Sensors and Systems for Space Applications II*, April 2008.

[17] T. Debus and S. Dougherty, "Overview and perrformance of the front-end robotics enabling near-term demonstratiion (FREND) robotic arm," *AIAA Aerospace Conference*, pp. 2009–1870, 2009.

[18] A. Parness, T. Hilgendorf, P. Daniel, M. Frost, V. White, and B. Kennedy, "Controllable on-off adhesion for earth orbit grappling applications," *IEEE Aerosapce Conference*, 2013.

[19] D. Santos, M. Spenko, A. Parness, S. Kim, and M. Cutkosky, "Directional adhesion for climbing: theoretical and practical considerations," *Journal of Adhesion Science and Technology*, vol. 21, no. 12-13, pp. 1317–1341, 2007.

[20] K. Autumn, A. Dittmore, D. Santos, M. Spenko, and M. Cutkosky, "Frictional adhesion: a new angle on gecko attachment," *Journal of Experimental Biology*, vol. 209, no. 18, pp. 3569–3579, 2006.